CRYSTAL GROWTH & DESIGN
2006
VOL. 6, NO. 8
1936−1941

Controlled Vapor−Liquid−Solid Growth of Indium, Gallium, and Tin Oxide Nanowires via Chemical Vapor Transport

M. C. Johnson,[†] S. Aloni,[‡] D. E. McCready,[§] and E. D. Bourret-Courchesne*,[†]

Materials Sciences Division, Lawrence Berkeley National Laboratory, and Molecular Foundry, Lawrence Berkeley National Laboratory, 1 Cyclotron Road, MS2R0200, Berkeley, California 94720-8197, and Department of Physics, University of California, Berkeley, California 94720, and Environmental Molecular Sciences Laboratory, Pacific Northwest National Laboratory, P.O. Box 999, MS K8-93, Richland, Washington 99352

Received October 6, 2005; Revised Manuscript Received March 31, 2006

ABSTRACT: We utilized a vapor−liquid−solid growth technique to synthesize indium oxide, gallium oxide, and tin oxide nanowires using chemical vapor transport with gold nanoparticles as the catalyst. Using identical growth parameters, we were able to synthesize single crystal nanowires typically 40−100 nm diameter and more than 10−100 μm long. The products were characterized by means of X-ray diffraction (XRD), scanning electron microscopy (SEM), and high-resolution transmission electron microscopy (HRTEM). All the wires were grown under the same growth conditions with growth rates inversely proportional to the source metal vapor pressure. Initial experiments show that different transparent oxide nanowires can be grown simultaneously on a single substrate with potential application for multicomponent gas sensors.

Introduction

One-dimensional nanostructures, such as wires, rods, belts, and tubes, have recently attracted much attention due to their novel properties and potential applications in nanoelectronics and nanophotonics.[1−6] Over the past decade, semiconductor 1D nanostructures such as carbon nanotubes, III−V, II−VI, Si−Ge, and oxides have been synthesized and studied for their nanoscale properties. Their reduced dimensionality leads to higher quality, defect-free material with high surface-to-volume ratio. The latter is now utilized in the construction of gas sensing devices when the surface properties are modified by adsorption of gas, which in turn affects the electronic properties of the wire. When the size of the nanowire is smaller than the exciton's Bohr radius in the bulk, the electronic properties are defined by the size due to quantum confinement effects. The metal oxides are extremely important technological materials for use in nanophotonic and nanoelectronic devices. Oxides, such as ZnO,[7] GeO_2,[8,9] In_2O_3,[10−12] SnO_2,[13] and Ga_2O_3,[14] have been synthesized into nanowire and nanobelt structures and were successfully integrated into numerous optoelectronic applications and nanoscopic gas sensors.[15−18]

The first step in utilization of nanostructures is the development of simple, reproducible, and controllable growth strategies for obtaining high-quality and high-purity materials. Many growth strategies have been employed to synthesize nanosized semiconducting oxides that have resulted in many different structures with various morphologies and properties. For instance, In_2O_3 nanowires have been grown using different vapor transport schemes utilizing various catalysts. Vapor−liquid−solid (VLS) mechanisms using catalytic Au thin films were utilized to obtain n-type In_2O_3 nanowires.[10] The In was delivered to the substrate via laser ablation of an InAs target, which requires expensive and specific equipment and apparatuses for synthesis. Zhang et al. used Ag catalyst and reduced In_2O_3 powders to obtain In_2O_3 nanowires.[11] The wires had a rough morphology and a wide size distribution (10−100 nm). More difficult techniques involved the electrodeposition of In nanowires using templates of anodic alumina membranes (AAMs), which involves a multistep process.[12] The In is then oxidized for as long as 12 h. Although this method allows for dense arrays of nanowires, the products have rough morphologies, and the synthesis involves many advanced processing steps and long annealing times. Tin oxide nanowires have been grown using self-catalytic thermal evaporation.[19−21] These self-catalytic methods result in single-crystal wires but with wide size distribution and various shapes. The self-catalytic process results in nanowires with rough morphology and leads to branching and dendritic growth.[20,21] High-quality SnO_2 wires have been obtained using electrochemical methods inside an alumina porous matrix.[22] Unfortunately this method takes a significant number of complex steps and involves long growth times. VLS techniques have also been reported for the synthesis of Ga_2O_3 nanowires.[14,23] Use of a thin layer of Au (25−100 Å) catalyst on Si substrates while flowing Ar carrier gas over heated Ga metal has resulted in high-purity, single crystal nanowires. This technique leads to nanowires having a diameter range of ∼80−350 nm.[14] Other VLS techniques use GaN as the Ga source while using In as the catalyst. This method produced single crystalline wires with a diameter range of 20−60 nm. One drawback is that this method uses another group III metal as a catalyst, which has potential for impurity substitution during synthesis. Other more advanced techniques use carbothermal reduction techniques[17] and metal−organic chemical vapor deposition.[24] These methods have complex chemistries and result in varying shapes and crystal quality. As just described, there are many different approaches for synthesis of oxide nanowires resulting in a wide variety of size, shape, and morphology. These growth techniques vary more widely when comparing synthesis of different material systems such as indium oxide, gallium oxide, and tin oxide. In this study, we demonstrate that the growth of In_2O_3, Ga_2O_3, and SnO_2 nanowires can be promoted

* Corresponding author. Phone: 1-510-486-5553. Fax: 1-510-486-5530. E-mail address: EDBourret@lbl.gov.
[†] Materials Sciences Division, Lawrence Berkeley National Laboratory.
[‡] Molecular Foundry, Lawrence Berkeley National Laboratory and Department of Physics, University of California, Berkeley.
[§] Environmental Molecular Sciences Laboratory, Pacific Northwest National Laboratory.

10.1021/cg050524g CCC: $33.50
Published on Web 07/08/2006

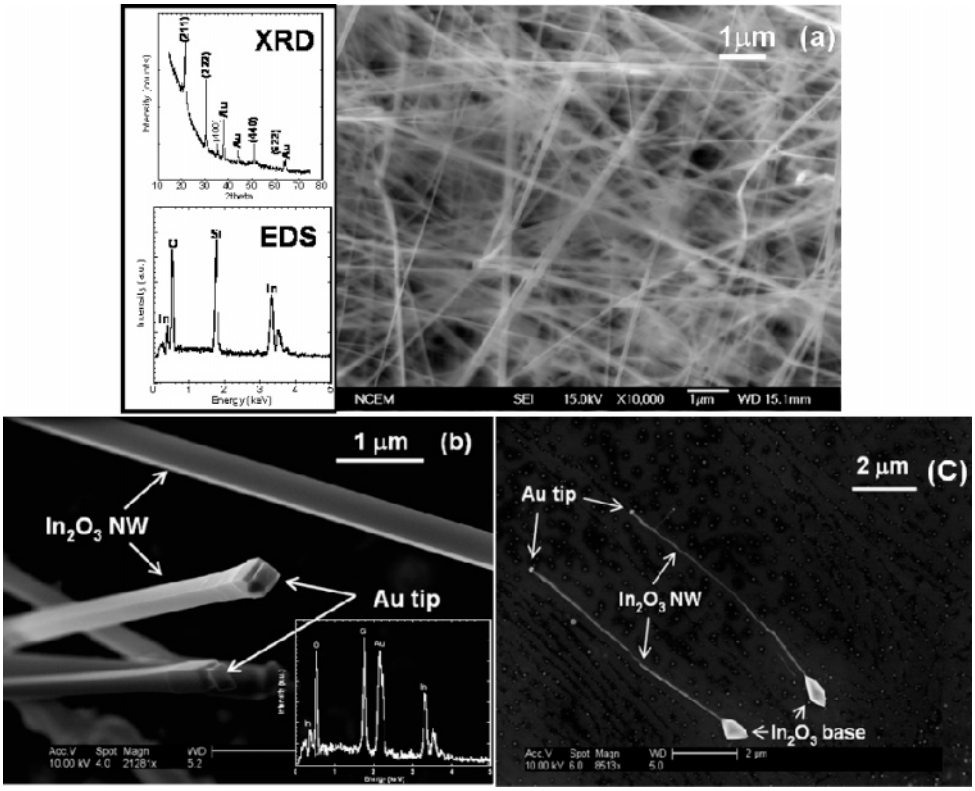

Figure 1. SEM analysis for In_2O_3 nanowires grown at 900 °C using Au catalyst: (a) low-magnification image of bulk nanowires—inset shows XRD spectrum with cubic phase material; EDS inset shows wires to consist of In and O only; Si peak is from the substrate; (b) high-magnification image of wires showing gold tips—Inset shows EDS spectrum taken at the tip verifying presence of Au; (c) low-magnification image of nanowires grown from large In_2O_3 octahedron base. These structures are formed due to a V−S growth mechanism as reported by Hao et al.[25]

by a simple, reproducible, and mutually compatible strategy using identical growth parameters. Our synthesis implements a VLS growth mechanism using gold nanoparticles as the catalyst. Finally, we show results of initial experiments that lead to simultaneous synthesis of In_2O_3 and SnO_2 nanowires on a single Si substrate.

Experimental Section

Substrates of Si(100) were cut into 10 mm × 10 mm squares and prepared by degreasing via sonication in trichloroethylene, acetone, methanol, and deionized water for 15 min each. Then the sample was dried using ultrapure N_2 and heated to approximately 110 °C. After being heated, a solution of 50 nm Au particles (Ted Pella, Inc.) with a mean diameter of 52.7 nm was dropped onto the substrate. The density of the Au particles varied depending on the amount of solution dropped onto the substrate. High-purity (6 N) metal reactant species (In, Ga, or Sn) were separately placed in a quartz boat and loaded into the center of a 25 mm fused quartz tube placed inside a horizontal tube furnace. Substrates were placed 2−5 mm downstream of the metal reactant species. The furnace was heated between 800 and 1000 °C (60 °C/min) under various flow rates of N_2 (100−1000 sccm), which contained sufficient amounts of oxygen precursors for synthesis. The nitrogen gas was supplied from the burnoff of a liquid nitrogen tank. The growth times varied between 0.5 and 3 h. Samples were cooled to room temperature under N_2 before being unloaded from the reaction furnace. Crystal structure and phase were defined using grazing incidence X-ray diffraction (GIXRD). Morphology and composition were determined using scanning electron microscopy (SEM) equipped with energy dispersive spectroscopy (EDS). Growth direction, crystallinity, and defect morphology were investigated using transmission electron microscopy (TEM) with nanobeam diffraction (NBD). The GIXRD apparatus was a Philips X'Pert MPD system equipped with a Cu source (λ = 1.5406 Å) and parallel beam optics. The incident beam angle (Ω) was fixed at 2.5°, the scan range was 15.00°−75.00° 2Θ, and the scan rate was 0.05°/45 s. Data analysis was accomplished using the software program JADE (Materials Data Inc., Livermore, CA) and the Powder Diffraction File database (International Centre for Diffraction Data, Newtown Square, PA). SEM was performed using a FEI Sirion 75 microscope equipped with an EDAX system, and high-resolution TEM (HRTEM) was performed using a JEOL 200 operating at 200 kV capable of NBD.

Results and Characterization

A. Indium Oxide Nanowires. Indium oxide nanowires were grown by placing high-purity indium in the center of a tube furnace at 900 °C and flowing N_2 as the carrier gas. Figure 1a shows a low magnification SEM image where there is a high density of long, straight nanowires. Typical lengths for these nanowires were 2−10 μm (dependent on growth time) with a radius of 50−100 nm giving an average growth rate of 4 μm/h. A typical XRD spectrum is attached to Figure 1a where the diffracted peaks are indexed and indicate cubic phase material. The strong intensities of the In_2O_3 peaks and the absence of any indium metal peaks indicate that the In_2O_3 nanowires were of high-purity, single-phase material. The lattice parameter was calculated to be a = 1.0115 nm, which is in good agreement with reported values (a = 1.0118 nm). The compositional purity of these nanowires was verified using EDS. A typical EDS spectrum is attached to Figure 1a, which shows that the individual nanowires consist of only In and O. The Si signal was from the substrate material. A high-magnification image is shown in Figure 1b. The nanowires have a very smooth morphology with a square cross-section. Compositional analysis at the tip of the nanowire (Figure 1b, inset) shows that it consists of In, O, and Au. The presence of a Au nanoparticle at the tip indicates that these nanowires are grown via a VLS growth mechanism. HRTEM images (Figure 2) reveal that a randomly selected In_2O_3 nanowire is very straight with a uniform diameter of 65 nm. The NBD pattern (inset, Figure 2b) confirms the XRD

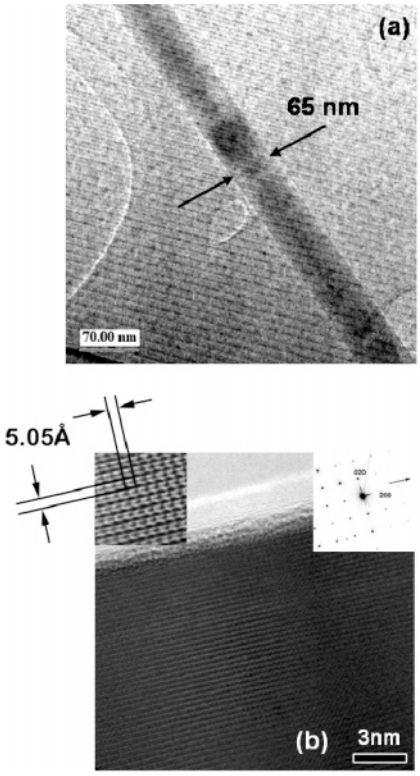

Figure 2. TEM analysis for In_2O_3 nanowires grown at 900 °C using Au catalyst: (a) low-magnification image of single nanowire with diameter of 65 nm and smooth surface morphology; (b) high-magnification image of defect-free nanowire. Insets show an atomically resolved image and a NBD spectrum indicating a growth direction of $\langle 100 \rangle$.

data that the nanowires are cubic In_2O_3 with a growth direction of $\langle 100 \rangle$. The high-resolution image shows defect-free material.

It is worth reporting that the growth of octahedral structures was found during some of the In_2O_3 nanowire synthesis runs although there was no change in growth conditions. Figure 1c shows a SEM image of some results that consist of Au tipped nanowires growing from large In_2O_3 octahedral bases. These octahedral structures were grown via a vapor−solid (VS) mechanism as reported by Hao et al.[25] and will be discussed later. EDS spectra of these structures showed the base and nanowire to be In_2O_3 with the tip being Au. This was not a common growth result. Most wires were grown perpendicular to the substrate surface without base formation.

B. Gallium Oxide Nanowires. To obtain Ga_2O_3 nanowires, the same growth conditions as those used for In_2O_3 nanowires were utilized except that high-purity Ga metal was used instead of In. The SEM image of the resulting Ga_2O_3 nanowires is shown in Figure 3a. The nanowires have average lengths greater than 20 μm with typical diameters between 40 and 50 nm. The inset shows a high magnification image of a nanowire with a diameter of 40 nm. The attached XRD spectrum reveals that the nanowires were monoclinic with lattice constants of a = 1.222 nm, b = 0.3041 nm, c = 0.5808 nm, and β = 103.8°. These values are in good agreement with reported bulk data (a = 1.227 nm, b = 0.3039 nm, c = 0.5808 nm, and β = 103.8°). The Ga_2O_3 nanowires had an average growth rate of 14 μm/h, which was 3 to 4 times greater than the In_2O_3 nanowires at the same growth conditions. Ga metal has a vapor pressure of 10^{-4} at 900 °C, which is 1.5 orders of magnitude lower than that of In metal at the same conditions. Thus the resulting increase in growth rate indicates that the growth is not limited by the metal vapor transport.

It is interesting to note that the Ga_2O_3 growth also contained structures consisting of triple junction wire nodes. Figure 3b shows a SEM image of a junction growth for the Ga_2O_3 nanowires. These junctions could be due to nucleation on twins or to the presence of a small Au particle on the wire. These junctions have widths and diameters greater than 1 μm and therefore were too thick to perform TEM.

Figure 3a shows the typical EDS spectrum for a Ga_2O_3 nanowire. The compositional makeup for the nanowires was Ga and O with no detection of any impurities above the detection limits with the exception of the Si substrate. EDS was also performed on the junction nodes of these wires with the same results. Figure 4a shows a TEM image of a single nanowire that is 40 μm long and 40 nm in diameter. The nanowire is extremely straight and smooth with a Au tip at the slightly tapered end as shown with the EDS spectrum in the inset. This indicates that the Ga_2O_3 nanowires were also grown via a VLS growth mechanism. Figure 4b shows a defect-free, high-resolution image of the nanowire with an interatomic spacing of c = 5.6 Å. The inset shows a NBD pattern, which confirms a single-crystal wire with a growth direction of $\langle 001 \rangle$.

C. Tin Oxide Nanowires. Tin oxide nanowires were also grown at the same growth conditions using high-purity tin metal. Figure 5 shows the results for a typical growth run of bulk nanowires. XRD analysis shown in Figure 5a shows that tin oxide nanowires were grown with the cassiterite (tetragonal) crystallographic configuration with lattice constants measured to be a = 0.4737 nm and c = 0.3185 nm, which is consistent with the bulk data (a = 0.4738 nm, c = 0.3187 nm). Figure 5a also shows the SEM and EDS results for the growth of tin oxide nanowires. The tin oxide nanowires are shown to be 50−75 nm in diameter with average lengths exceeding 50 μm. This corresponds to an average growth rate of approximately 20 μm/h. These wires are smooth with constant diameters for the length of the wires. The EDS analysis shows that the wires consist of Sn and O with no evidence of impurity detection.

The HRTEM verified that the morphology of the nanowires was extremely smooth and the diameter is constant along the length of these wires (Figure 5b). The insets show that the nanowires were single crystalline. NBD analysis verifies that the tin oxide nanowire has a growth direction of $\langle 100 \rangle$, and the interatomic spacing was 4.7 Å, which is consistent for cassiterite SnO_2. These data show the SnO_2 nanowires to be high-quality, defect-free material.

Discussion

Growth parameter conditions have been established to synthesize single-crystal In_2O_3, Ga_2O_3, and SnO_2 nanowires. Structural and morphological characterization showed the nanowires to be extremely high-quality and defect-free. These results show that all three types of wires are extremely smooth, which is not always consistent in the literature for oxide nanowires.[11−13,24,25] Compositional analysis showed the tips to consist of gold nanoparticles saturated with metal and oxygen atoms, which is consistent with a VLS growth mechanism. Table 1 gives a summary of physical and growth parameters for nanowires synthesis. The nanowire diameters are relatively constant where the diameter of the resulting wire is dependent on the size of nanoparticle catalyst used. The diameters for all three systems range between 40 and 100 nm, which is consistent with the size of catalyst used for our synthesis (nominal 50 nm Au nanoparticles). There is some range in diameter due to the aggregation of Au nanoparticles.

The average Au catalyst particle was advertised as 52.7 nm as determined by the vendor. It was found that the average

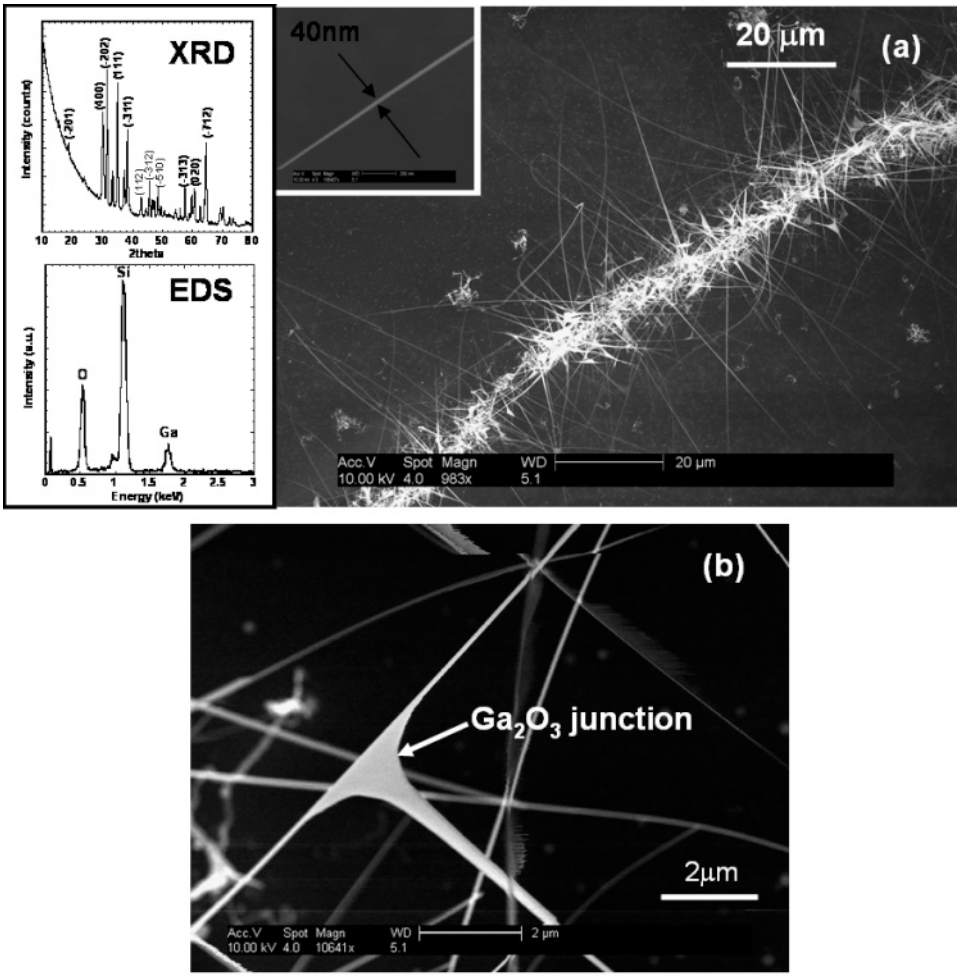

Figure 3. SEM analysis for Ga_2O_3 nanowire grown at 900 °C using Au catalyst: (a) low-magnification image showing bulk wires with lengths exceeding 20 μm—inset is a high-magnification image of single wire with diameter of 40 nm; side insets include XRD and EDS spectra showing single phase monoclinic material consisting of only Ga and O; (b) high-magnification image showing junction node of Ga_2O_3 nanowire.

diameter size ranged from 50 to 100 nm for In_2O_3, 40−60 nm for Ga_2O_3, and 50−100 nm for SnO_2. The larger diameter nanowires were determined to be due to catalyst particle aggregation. As the temperature was increased to 900 °C, surface mobility of the catalyst particles increased while the surfactant was being burned off. This allows the catalyst particles to agglomerate into larger size particles. Experiments were conducted to decrease the density of particles on the surface by diluting the catalyst solution with different diluents (deionized H_2O, methanol, acetone) to different concentrations. This was done in the hope of decreasing the chance of particles aggregating at the higher temperatures. It turns out that larger diameter wires were still grown using the lowest particle concentrations (1:10 by volume) that still allow for acceptable amounts of nanowire synthesis. Other techniques are needed for controlled catalyst deposition, which will have a more controlled effect on diameter size, which is beyond the scope of this paper.

While the In_2O_3 synthesis produced mainly single-crystal nanowires, Figure 1c shows the growth of two octahedron In_2O_3 structures forming the base of nanowires. The octahedron structures are large, with sizes on the order of 1 μm. EDS and XRD analysis also shows that these structures consist of only cubic In_2O_3 without the presence of any catalyst material. Therefore it is believed that these structures are formed by a VS growth mechanism instead of the VLS growth mechanism that forms nanowires. Hao et al. report In_2O_3 octahedron CVD growth using In metal and Ar carrier gas on Si substrates.[25] They describe this growth as a vapor−solid mechanism and analyze the products in terms of surface energies resulting in different sizes and shapes. They also describe the synthesis of imperfect octahedrons due to long growth times (>2 h) and attribute this effect to structural defects such as oxygen vacancies, indium interstitials, oxygen interstitials, and oxygen antisite defects. Our results agree very well with their reported results. The shapes of our octahedron bases are imperfect due to the long growth times used for growth of the nanowires. Also, it was determined that these octahedron structures were not due to a catalyst-mediated growth mode, verifying a VS growth mechanism.

We found that the growth rate of these nanowires increases in the order of In_2O_3, Ga_2O_3, and SnO_2, respectively. This is inversely proportional to the vapor pressure of the respective reactant metal species at the growth temperature. As the vapor pressure of the metal reactant increases, the growth rate of the nanowire decreases as depicted in Figure 6. This increased metal vapor pressure causes an increased suppression of the already limited oxygen content in the N_2 carrier gas, which, in turn, limits the transport of oxygen vapor to the growing catalyst interface. Therefore the limiting reactant in these growing nanowires is the small amount of residual oxygen, which is supplied from the flowing nitrogen. One possible way to control and optimize the growth rate is to supply a diluted O_2/inert gas mixture. Our experiments show that large amounts of oxygen at high growth temperatures induce rapid oxidation of the

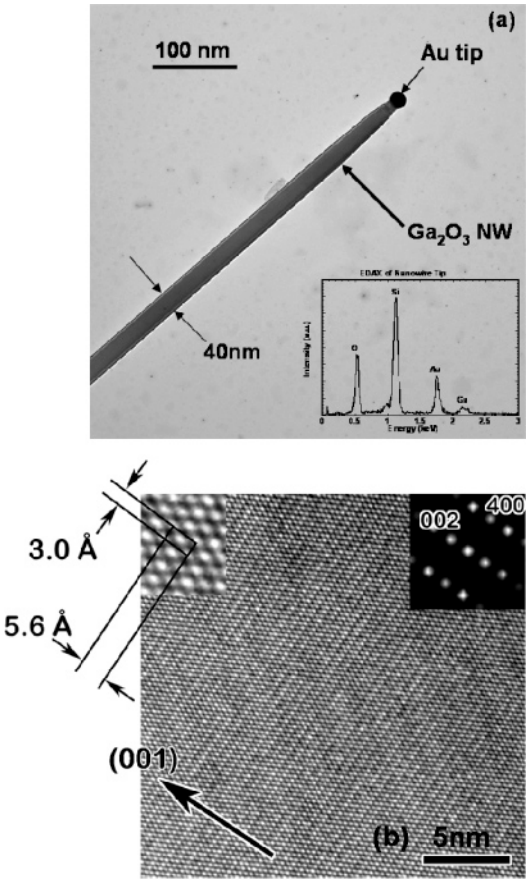

Figure 4. TEM analysis for Ga_2O_3 nanowires grown at 900 °C using Au catalyst: (a) low-magnification image of single nanowire with a diameter of 40 nm with a metal tip—the inset shows an EDS spectrum of the tip of the nanowire verifying that the tip consists of gold catalyst; (b) high-magnification image of defect-free nanowire—insets show an atomically resolved image and a NBD spectrum indicating a growth direction of ⟨002⟩ .

Table 1. Growth Parameters and Physical Properties of In_2O_3, Ga_2O_3, and SnO_2 Nanowires Grown via a VLS Mechanism Using Metal Vapor Transport for a 30 min Growth Time

parameter	In_2O_3	Ga_2O_3	SnO_2
growth temperature (°C)	900	900	900
catalyst	50 nm Au	50 nm Au	50 nm Au
N_2 flow rate (sccm)	500	500	500
diameter (nm)	50−100	40−60	50−100
average growth rate (μm/h)	4	14	20
metal vapor pressure (Torr)	3×10^{-3}	1×10^{-4}	3×10^{-5}
crystalline phase	cubic	monoclinic	tetragonal

reactant metal, which results in an oxide coating. This, in turn, prevents the evaporation of the metal reactant source.

The growth times for the synthesis of different oxide nanowires varied between 0.5 and 3 h. The synthesis of all three oxide nanowires showed consistent kinetic data for all growth times. The increase in growth time only resulted in an increase in nanowire length with diameters remaining constant. This is further proof that the diameter of nanowire is dependent on catalyst particle size. More importantly, there were no changes in crystallinity or morphological properties with wire length (i.e. growth time). Experiments were conducted a minimum of five times and showed a consistent reproducibility in growth and structural properties. This simple and reproducible synthesis technique of high-quality nanowires implies an attractive method for future development of multicomponent oxide nanowire devices.

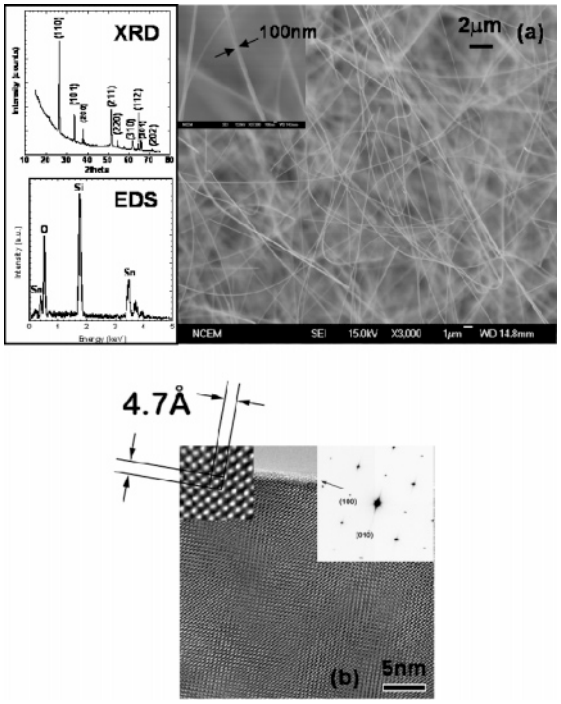

Figure 5. SEM and TEM analysis for SnO_2 nanowires grown at 900 °C using Au catalyst: (a) low-magnification SEM image of long, smooth nanowires—inset shows a smooth nanowire with a diameter of 100 nm; side insets include XRD and EDS spectra showing single phase tetragonal material consisting of only Sn and O; (b) high-magnification TEM image of defect-free nanowire—insets show an atomically resolved image and a NBD spectrum indicating a growth direction of ⟨100⟩ .

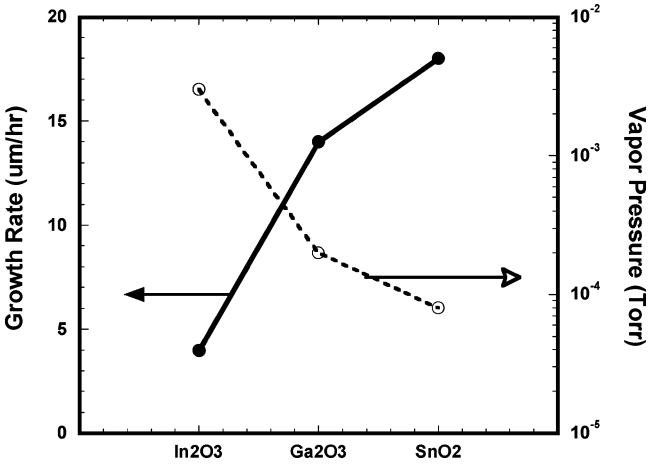

Figure 6. Comparison of growth rate and metal vapor pressure for all three metal oxide nanowires.

Initial experiments were performed for the growth of multiple types of nanowires on a single substrate. By simultaneously flowing In and Sn metal vapor at the same growth conditions used for single type wire growth (900 °C, 500 sccm N_2, 50 nm Au catalyst) a dual growth mode was achieved. Formation of In_2O_3 and SnO_2 nanowires on a single substrate was confirmed by XRD. Diffraction data showed peaks for both cubic In_2O_3 and tetragonal SnO_2 wires, which verifies that they exist separately, while there was no diffraction peaks for ternary indium tin oxide nanowires. These initial experiments show the potential for simultaneously growing oxide nanowires on a single substrate at a single growth condition. Research is being performed on the development of controlled growth of multiple wire types as well as the ternary compounds.

Conclusion

A simple VLS growth strategy has been developed to synthesize high quality In_2O_3, Ga_2O_3, and SnO_2 nanowires. All three oxide nanowire systems can be grown under identical conditions using a gold catalyst material. Structural and morphological characterizations have shown that the nanowires are single crystal with extremely smooth morphologies. The diameters range from 40 to 100 nm with lengths from several micrometers to over 50 μm. It has been shown that the growth rate of the different nanowires is inversely proportional to the vapor pressure of the respective metal reactant species. This is due to the displacement of oxygen precursor as the metal reactant vapor pressure increases. These nanowires can be grown simultaneously on a single substrate, which has potential uses for multicomponent gas-phase detection. It also implies that ternary or doped materials can be grown using simple CVD methods.

Acknowledgment. This work was supported by the Director, Office of Science, Office of Basic Energy Sciences, Division of Materials Science and Engineering, of the U.S. Department of Energy under Contract No. DE-AC02-05CH11231. The research described in this paper was performed [in part] in the Environmental Molecular Sciences Laboratory, a national scientific user facility sponsored by the U.S. Department of Energy's Office of Biological and Environmental Research and located at Pacific Northwest National Laboratory in Richland, WA.

References

(1) Iijima, S. *Nature (London)* **1991**, *354*, 56.
(2) Kong, J.; Zhou, C.; Morpurgo, A.; Soh, H. T.; Quate, C. F.; Marcus, C.; Dai, H. *Appl. Phys. A* **1999**, *69*, 305.
(3) Hu, J. T.; Odom, T. W.; Lieber, C. M. *Acc. Chem. Res.* **1999**, *32*, 435.
(4) Cui, Y.; Lauhon, J.; Gudiksen, M. S.; Wang, J.; Lieber, C. M. *Appl. Phys. Lett.* **2001**, *78*, 2214.
(5) Duan, X.; Lieber, C. M. *J. Am. Chem. Soc.* **2000**, *122*, 188.
(6) Xia, Y.; Yang, P.; Sun, Y.; Wu, Y.; Mayers, B.; Gates, B.; Yin, Y.; Kim, F.; Yan, H. *Adv. Mater.* **2003**, *15*, 353.
(7) Huang, M. H.; Wu, Y.; Feick, H.; Tran, N.; Weber, E.; Yang, P. *Adv. Mater.* **2001**, *13*, 113.
(8) Wu, X. C.; Song, W. H.; Pu, M. H.; Zhao, B.; Sun, Y. P.; Du, J. J. *Chem. Phys. Lett.* **2001**, *349*, 210.
(9) Bai, Z. G.; Yu, D. P.; Zhang, H. Z.; Ding, Y.; Wang, Y. P.; Gai, X. Z.; Hang, Q. L.; Xiong, G. C.; Feng, S. Q. *Chem. Phys. Lett.* **1999**, *303*, 311.
(10) Li, C.; Zhang, D.; Han, S.; Liu, X.; Tang, T.; Zhou, C. *Adv. Mater.* **2003**, *15*, 143.
(11) Zhang, J.; Qing, X.; Jiang, F.; Dai, Z. *Chem. Phys. Lett.* **2003**, *371*, 311.
(12) Zheng, M. J.; Zhang, L. D.; Li, G. H.; Zhang, X. Y.; Wang, X. F. *Appl. Phys. Lett.* **2001**, *79*, 839.
(13) Dai, Z. R.; Gole, J. L.; Stout, J. D.; Wang, Z. L. *J. Phys. Chem. B* **2002**, *106*, 1274.
(14) Guha, P.; Chakrabarti, S.; Chaudhuri, S. *Physica E* **2004**, *23*, 81.
(15) Li, C.; Zhang, D.; Liu, X.; Han, S.; Tang, T.; Han, J.; Zhou, C. *Appl. Phys. Lett.* **2002**, *82*, 1613.
(16) Zhang, D.; Li, C.; Liu, X.; Han, S.; Tang, T.; Zhou, C. *Appl. Phys. Lett.* **2003**, *83*, 1845.
(17) Wu, X. C.; Song, W. H.; Huang, W. D.; Pu, M. H.; Zhao, B.; Sun, Y. P.; Du, J. J. *Chem. Phys. Lett.* **2000**, *328*, 5.
(18) Law, M.; Kind, H.; Kim, F.; Messer, B.; Yang, P. *Angew. Chem., Int. Ed.* **2002**, *41*, 2405.
(19) Ramgir, N. S.; Mulla, I. S.; Vijayamohanan, K. P. *J. Phys. Chem. B* **2004**, *108*, 14815.
(20) Chen, Y.; Cui, X.; Zhang, K.; Pan, D.; Zhang, S.; Wang, B.; Hou, J. G. *Chem. Phys. Lett.* **2003**, *369*, 16.
(21) Ma, Y. J.; Zhou, F.; Lu, L.; Zhang, Z. *Solid State Commun.* **2004**, *130*, 313.
(22) Zhang, Y.; Kolmakov, A.; Chreitien, S.; Metiu, H.; Moskovits, M. *Nano Lett.* **2004**, *4*, 403.
(23) Zhang, J.; Jiang, F. *Chem. Phys.* **2003**, *289*, 243.
(24) Kim, H. W.; Kim, N. H. *Appl. Surf. Sci.* **2004**, *233*, 294.
(25) Hao, Y.; Meng, G.; Ye, C.; Zhang, L. *Cryst. Growth Des.* **2005**, *5*, 1617.

CG050524G